Article

Illuminating Disorder Induced by Glu in a Stable Arg-Anchored Transmembrane Helix

Jake R. Price, Fahmida Afrose, Denise V. Greathouse, and Roger E. Koeppe, II*

Read Online

ACCESS | Metrics & More | Article Recommendations | SI Supporting Information

ABSTRACT: Membrane proteins are vital for biological function and are complex to study. Even in model peptide-lipid systems, the combined influence or interaction of pairs of chemical groups still is not well understood. Disordered proteins, whether in solution or near lipid membranes, are an emerging paradigm for the initiation and control of biological function. The disorder can involve molecular orientation as well as molecular folding. This paper reports an astonishing induction of disorder when one Glu residue is introduced into a highly stable 23-residue transmembrane helix. The parent helix is anchored by a single Arg residue, tilted at a well-defined angle with respect to the DOPC bilayer normal and undergoes rapid cone precession. When Glu is introduced two residues away from Arg, with 200° (or 160°) radial separation, the helix properties change radically to exhibit a multiplicity of three or more disordered states. The helix characteristics have been monitored by deuterium (^{2}H) NMR spectroscopy as functions of the pH and lipid bilayer composition. The disordered multistate behavior of the (Glu, Arg)-containing helix varies with the lipid bilayer thickness and pH. The results highlight a fundamental induction of protein multistate properties by a single Glu residue in a lipid membrane environment.

E16 with R14   R14 alone

40 kHz 0 -40   60 kHz 0 -60
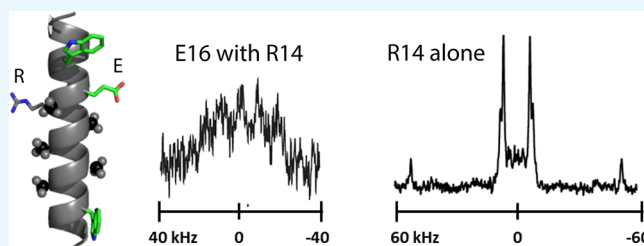
INTRODUCTION

While a distinctively folded protein structure was an early paradigm for understanding protein function[1] and enzyme activity,[2] over time, the importance of disordered protein domains increasingly has been recognized and appreciated.[3,4] By the year 2000, about 91 proteins were known to be "natively unfolded" or "intrinsically disordered",[5] and the number of domains or whole proteins identified as disordered has only continued to grow at a rapid pace. Indeed, the abundance and functional significance of protein disorder in eukaryotes now are well established.[6,7] The functional importance is highlighted by the observation that many eukaryotic proteins contain both structured and disordered regions.[6] The disorder can involve changes in molecular recognition as well as small or large changes in backbone folding, local or global. Disordered proteins and multisite recognition play central roles in protein interaction networks, in the regulation of cell signaling, and in the ordered assembly of macromolecular complexes such as ribosomes, chromatin, and microfilaments.[6] As such, single-residue mutations within disordered domains may be associated with human disease. To this end, it is important to understand fundamental systems wherein a single-residue change may influence protein disorder.

Intrinsically disordered proteins or protein domains are characterized by low sequence complexity and a low content of bulky hydrophobic amino-acid residues. Rather than folding into a well-defined globular structure, a disordered domain fluctuates rapidly over an ensemble of conformations.[6] The

molecular interactions with small or large binding partners are transient and dynamic. A multiplicity of interaction motifs brings forward advantages for signaling. The content and distribution of charged residues exert profound influence for such interactions[6] such that changes in net charge or charge distribution strongly guide conformational propensities and binding partner recognition events.

The landscape of membrane proteins also embraces protein disorder in terms of not only global folding but also local unwinding, binding interactions, and molecular recognition. Disordered proteins are featured in key aspects of physiology such as signaling and membrane trafficking, highlighted by their remarkable specificity for binding diverse biological membranes.[8] A disordered domain may gain a structure, in particular the helical structure, upon membrane binding. Binding specificity is encoded partly in the primary sequence and can be modified by single mutations or post-translational modifications.[8,9] As such, single-site changes can be highly relevant for regulating the protein disorder.

Within the above context, it remains difficult fundamentally to predict the consequence of a single modification for the
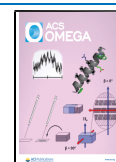
protein multistate behavior. Below, we report dramatic results when a single positively charged residue is joined by a negative residue near a lipid membrane interface. We will briefly describe the background properties of the parent peptide's helical framework and then will introduce and assess experimentally the mutation that causes the multistate properties.

The hydrophobic peptide GWALP23 (acetyl-GGALW^{5}LALALALALALALW^{19}LAGA-amide) spans a lipid bilayer as a transmembrane helix while exhibiting low to moderate dynamic averaging and a helix tilt angle that scales with the bilayer thickness to satisfy hydrophobic matching principles.[10,11] Several features contribute to the orientation and dynamic properties of such a helix. An isolated helix undergoes rapid rotational averaging about the bilayer normal, as evidenced by the solid-state NMR spectra of oriented samples when aligned with the bilayer normal perpendicular to the magnetic field.[12,13] This universal "first-level" dynamic averaging for a well-oriented helix has been described as cone "precession", which confers an advantageous rotational entropy that favors a finite non-zero helix tilt angle τ_0.[14] Additional dynamic properties include a "wobble" ($\sigma\tau$) of the helix about the finite tilt angle and a rotational "slippage" ($\sigma\rho$) about the axis of the tilted helix.[15,16]

In the above framework, many transmembrane helices have shown a small wobble $\sigma\tau$ of about 5−10°. The parent helix of GWALP23 exhibits such wobble and additionally an azimuthal slippage $\sigma\rho$ in a moderate range of 40−50°.[16] When R14 is introduced (Table 1), the ^{2}H NMR spectra sharpen, the helix

Table 1. Sequences of Peptides

name	sequence[a]	reference
GWALP23	acetyl-GGALWLALALALAL^{14}ALALWLAGA-amide	11
R^{14}GWALP23	GGALWLALALALAR^{14}ALALWLAGA	17
E^{16}GWALP23	GGALWLALALALALAE^{16}ALWLAGA	20
R^{14}E^{16}GWALP23	GGALWLALALALAR^{14}AE^{16}ALWLAGA	this work

[a]All of the peptide terminals are blocked with N-acetyl and C-amide groups. The parent sequence of GWALP23 has no charges.

tilt τ_0 increases by about 10°, the bilayer exhibits local thinning, the mean azimuthal rotation ρ_0 about the helix axis changes by about 80°, providing the R14 guanidinium group access to the membrane interface, and $\sigma\rho$ decreases below 30°.[17−19]

Given the stable properties of the parent uncharged GWALP23 helix in lipid bilayers and the dramatic changes when R14 is introduced, we sought to investigate the consequences of E16 on an opposite face of the helix. As a further background, E16 alone confers spectral broadening with little or no pH dependence for the core helix orientation yet significant local unwinding at high pH.[20] We now examine the influence of E16 upon the very stable Arg-anchored R14 helix, acetyl-GGALW^{5}LALALALAR^{14}ALALW^{19}LAGA-amide, in bilayer membranes. Notably, the Glu residue is placed on the opposite face of the helix from that of the Arg residue, with 200° (or 360−200°) radial separation (Figure 1). The goal of this work is to uncover and understand the combined influence of the single Glu and Arg residues near a membrane interface for the lipid interactions of the transmembrane helix. The results will reveal benchmarks to guide understanding of the
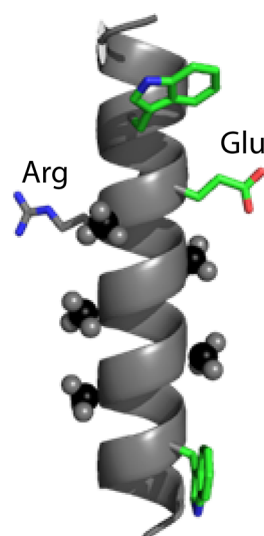

Figure 1. Model of R^{14}E^{16}-GWALP23, highlighting the Trp (W) indole rings and the Arg (R) guanidino and Glu (E) carboxyl side chains, with 200° radial separation of R from E. The space-filling methyl groups depict the deuteration sites on five of the six Ala residues of the core helix.

membrane protein structural order and the importance of molecular interactions at the lipid interface.

RESULTS

The mere introduction of glutamic acid E16 causes disorder for the otherwise very stable transmembrane helix of R^{14}GWALP23. The ^{2}H NMR spectra for labeled alanines in the core helix of R^{14}GWALP23 show extremely sharp resonances, revealing moreover resonances for some of the C_α deuterons (Figure 2), which typically are problematic to
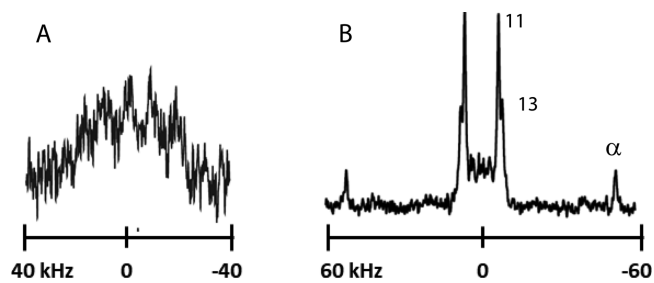

Figure 2. Deuterium NMR spectra illustrating the influence of E16 replacing L16 in R^{14}GWALP23 in DOPC. Spectra are shown for ^{2}H-labeled alanines A11 and A13 in oriented samples of R^{14}X^{16}GWALP23 in DOPC bilayers, hydrated at pH 6.4, where X is (A) Glu or (B) Leu. Sample orientation $\beta = 0°$; 1:60, peptide:lipid; 50 °C. The spectrum (B) has been reproduced from ref 17.

detect unless both the molecular alignment and the macroscopic sample alignment are exquisitely good.[19] In stark contrast, the introduction of E16 causes an array of molecular disorder that is revealed in the NMR spectra (Figure 2A). The immediate revelation is that the target helix with E16 and R14 occupies a multiplicity of states with respect to the DOPC membrane.

The findings of molecular and spectral disorder were confirmed with measurements in different lipid membranes and by varying the pH. In bilayer membranes of DLPC or DMPC, the peptide helix is more ordered and adopts a major
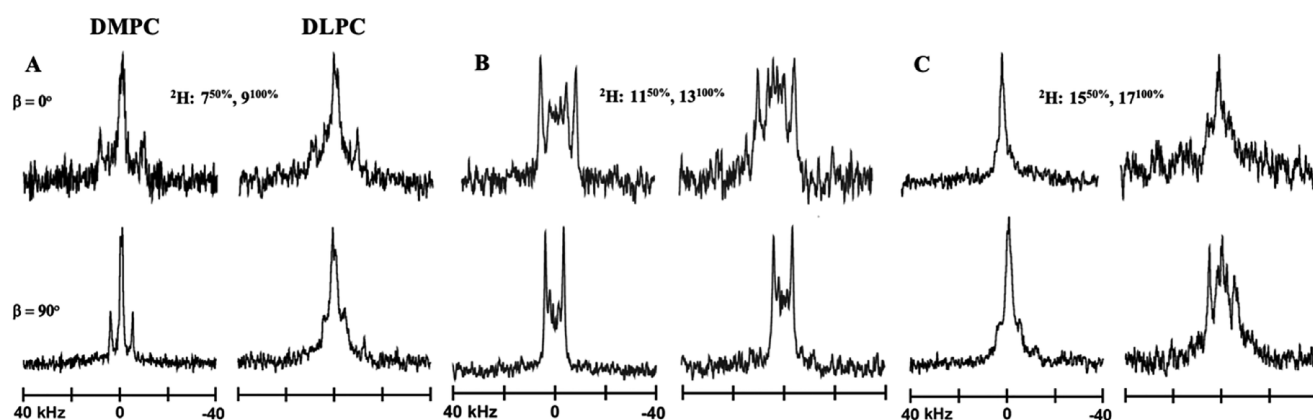
Figure 3. Deuterium NMR spectra of R^{14}E^{16}GWALP23 in DMPC (left) and DLPC (right) with ^{2}H-labeled alanines A7 and A9 (A), A11 and A13 (B), and A15 and A17 (C), shown for $\beta = 0°$ (upper) and $\beta = 90°$ (lower) sample orientations; pH 6.4, 50 °C; 1:60, peptide:lipid.

Table 2. Deuterium Quadrupolar Splittings in kHz for ^{2}H-Labeled Ala Side Chains in GWALP23 Peptides, Oriented in Lipid-Bilayer Membranes, with Variable Residues at Positions 14 and 16[a]

residue ID[b]				Ala CD$_3$ quadrupolar splittings in kHz[a]						
14	16	lipid	pH	A7	A9	A11	A13	A15	A17	ref
L	L	DLPC	--[c]	26.4	25.5	26.9	14.6	20.7	3.4	11
R	L	DLPC	--[c]	33.0	21.1	25.7	9.3	6.8	30.8	19
L	E	DLPC	6.1	13.0	5.0	19.2	13.4	21.4	14.2	20
R	E	DLPC	6.4	18.3	1.7	7.1	14.6	1.6	17.2	this work
L	L	DMPC	--[c]	21.9	8.9	20.9	3.8	17.6	2.9	11
R	L	DMPC	--[c]	30.6	14.1	21.3	10.3	3.7	29.1	19
L	E	DMPC		--[d]	--	--	--	--	--	20
R	E	DMPC	6.4	17.3	2.2	6.6	15.0	2	18	this work
L	L	DOPC	--[c]	16.6	1.7	16.7	1.5	15.4	2.6	11
R	L	DOPC	--[c]	26.6	5.5	16.0	13.1	1.3	28.0	17
L	E	DOPC	6.1	N.A.[e]	N.A.	N.A.	N.A.	N.A.	N.A.	20
R	E	DOPC	8.5	--	--	37	37	--	--	this work
R	E	DOPC	6.4	N.A.[e]	N.A.	8, 12, 28, 37, 50		N.A.	N.A.	this work
R	E	DOPC	4.9	--	--	4, 20, 37, 42, 62			--	this work
R	E	DOPC	4.5	--	--	--	--	2, 6	26, 40	this work
R	E	DOPC	3.3	--	--	3, 19, 37, 41, 62		--	--	this work
R	E	DOPC	2.4	--	--	3	20	2	25	this work

[a]The values reported in kHz are for a $\beta = 0°$ sample orientation. [b]Residues 14 and 16 are Leu in the parent sequence of acetyl-GGALW(LA)$_6$LWLAGA-amide. These were changed to R14 and/or E16 as noted. [c]Unbuffered at neutral pH. The peptide helix with leucine L14 and L16 has no ionizable groups. The peptide helix with R14 and L16 is not sensitive to pH.[23] [d]Values not listed (--) were not measured. [e]Not applicable (N.A.). Individual peaks could not be assigned in the broad ^{2}H NMR spectra.

transmembrane configuration at neutral pH (Figure 3), contrasting with the situation in DOPC. The NMR spectra in Figure 3 indicate a major well-defined molecular population in each bilayer membrane, characterized by the ^{2}H quadrupolar splittings that are listed in Table 2. The major population in DMPC or DLPC consists of a transmembrane helix that is tilted much less than when R14 is present alone without E16. The helix orientation is essentially the same in DLPC and DMPC, with a tilt of about 10° from the bilayer normal and an azimuthal rotation that differs by about 25° from the value observed when R14 is present alone without E16 (Figure 4). When a sample is turned from $\beta = 0°$ to $\beta = 90°$, a factor of 2 reduction is observed for the magnitude of the ^{2}H quadrupolar splitting $|\Delta\nu_q|$ (Figure 3), indicative of rapid precession[14,21] of the tilted helix about the DLPC or DMPC bilayer normal. The changes to the transmembrane helix orientation, including the tilt of the helix axis and azimuthal rotation around the axis, when first R14 and then also E16 are introduced, are illustrated by the fits to the deuterium quadrupolar wave plots in Figure 4.

Because the helix of R^{14}E^{16}GWALP23 is disordered in DOPC at neutral pH, we sought to examine the helix behavior when the pH is changed. Unless the pH is very low, multiple disordered states are observed. At pH 2.4, nevertheless, the predominant transmembrane helix orientation in DOPC can be compared with the results observed in DLPC and DMPC. As shown in the lower panel of Figure 4, the R^{14}E^{16}GWALP23 helix at pH 2.4 in DOPC is tilted to a similar extent (about 10°) as in DLPC or DMPC yet is rotated by an additional 20° about the helix axis (see also Table 3). If we summarize the rotational trends, starting from the parent helix of GWALP23, then the presence of R14 alters the azimuthal rotation of the transmembrane helix by about 45° in DLPC, 55° in DMPC, and 75° in DOPC (Table 3). Then, the further introduction of residue E16 continues these trends (in the same rotational direction) by an additional 25° in DLPC, 20° in DMPC, and 35° in DOPC (Table 3). The endpoint is a similar rotation of the R^{14}E^{16}GWALP23 helix in DLPC and DMPC but a value that is about 20° different in DOPC (when the helix
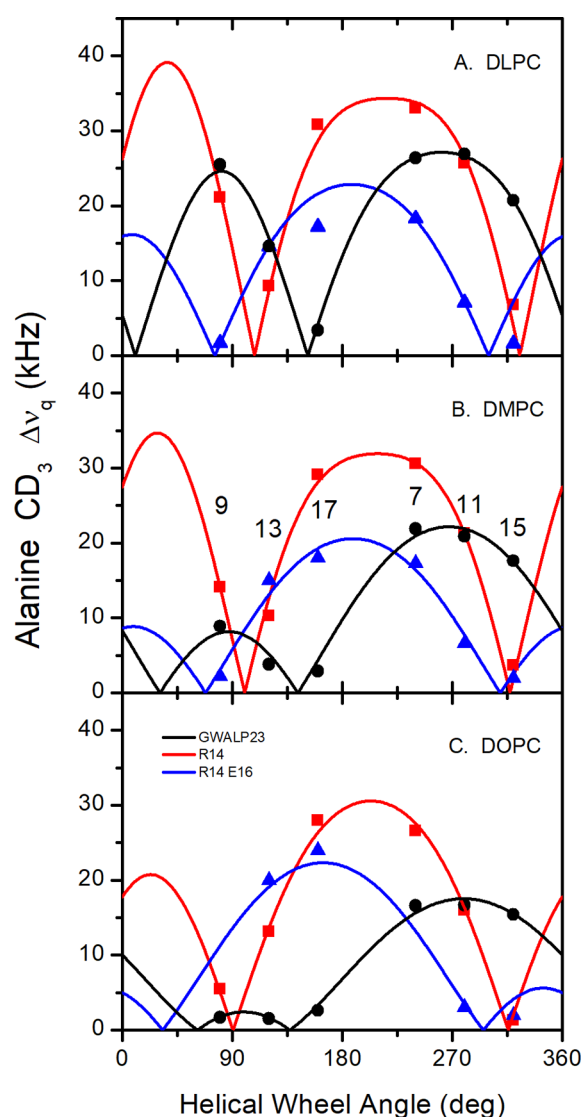
Figure 4. Quadrupolar wave plots of R^{14}E^{16}GWALP23 (blue) compared to R^{14}GWALP23 (red) and GWALP23 (black) in bilayers of DLPC (A) or DMPC (B) at neutral pH or DOPC (C) at low pH. The respective pH values for the R^{14}E^{16}GWALP23 samples are 6.4 (A), 6.4 (B), and 2.4 (C). The identities and radial locations of the ^{2}H-labeled Ala residues are indicated in panel (B). In DOPC, the R^{14}E^{16}GWALP23 helix adopts a major defined orientation only at low pH (see text). The spectra for GWALP23 and R^{14}GWALP23 are independent of pH.[22,23]

orientation can be deciphered, at low pH). Remarkably, the helix tilt is about the same as all three membranes.

As the pH is raised in DOPC membranes, dramatic changes are observed. Already at pH 3.5, multiple ^{2}H NMR peaks are evident (Figure 5). Between pH 3.5 and 8, the R^{14}E^{16}GWALP23 helix in DOPC is characterized by disorder involving multiple low-occupancy states without a dominant preferred orientation or location for the helix. While some of the quadrupolar splittings can be measured, it is impossible to know the number of states giving rise to the NMR spectra. From two ^{2}H-labeled alanines, one detects at least six sets of quadrupolar splittings, as compiled in Table 2, with additional low-intensity peaks also manifesting in Figure 5. Disorder among many low-level states is the order of the day.

As the pH is raised above pH 2.4, the dominant state for the helix in DOPC at low pH exists in equilibrium with an assortment of many other states. Because of the multistate properties as opposed to a two-state transition, the pH dependence does not describe a true titration behavior. A similar situation has been treated for residue K12 in GWALP23, which confers multistate properties for the helix in DOPC when the Lys side chain is charged.[22] In a similar fashion, one can estimate the pH dependence for losing the major low-pH population for the R^{14}E^{16}GWALP23 helix as residue E16 releases a proton and assumes a negative charge when the pH is raised. Although not a two-state equilibrium and not a true titration curve, one observes that one of the high-pH states for R^{14}E^{16}GWALP23 is 50% populated at about pH 4.5 (see Figure S3 of the Supporting Information). Because the major state at low pH interconverts with multiple and incompletely defined states at pH 4.5, the major population when E16 is neutral will exceed the occupancy of any individual state when E16 is ionized at pH 4.5 (see also ref 22). The midpoint for changes in a ^{2}H NMR peak intensity therefore constitutes only an estimate for the pK_a of E16 in R^{14}E^{16}GWALP23. The pH dependence can be attributed to the Glu residue (E16) because Arg (R14) remains charged throughout the pH range,[22,23] and no other titratable groups are present. A relatively standard titration range with a midpoint somewhat near 4.5 for glutamic acid residue E16 is consistent with a relatively polar environment involving perhaps aqueous access and/or proximity to the positively charged R14 side chain. At still a higher pH, further transitions occur as the multiple states coalesce toward an endpoint that appears in the form of a Pake pattern at a pH of about 8 (Figure 5), reflecting immobilization that could be caused by peptide aggregation or other factors. The complexities depend upon the presence of both residues E16 and R14.

■ DISCUSSION

Protein disorder involving multiple states has important functional consequences, for example among activation domains for transcription and chaperones for protein folding,[7] among others. In the realm of membrane proteins, locally disordered domains may regulate signal transduction by influencing the activation of key receptors.[24,25] Membrane binding of disordered domains, such as that of α-synuclein,[8] may lead not only to membrane remodeling and the promotion of normal functions such as neurotransmitter release but also in some cases of diseased states such as Parkinson's disease.[8] The sensing of membrane curvature and regulation of synaptic vesicle fusion are influenced by order/disorder transitions, as is protein aggregation. While such transitions in turn may relate to specific mutations, tyrosine phosphorylation, and helix/broken helix transitions,[8] the detailed molecular interactions that are responsible for local or global changes are not yet fully comprehended. Single-site consequences for the regulation of order/disorder transitions need to be better understood.

The resulting protein and lipid interactions may have functional repercussions. An important instance is a key Arg-Glu interaction that stabilizes a recognition domain of an essential chaperone for proper intracellular trafficking of the crucial cardiac Na$_v$1.5 channel.[26] Mutation of Glu to Asp in the chaperone, or of Arg to Gln, or mutation of nearby Asp or Ser residues, leads to cell surface accumulation of Na$_v$1.5 and may cause Brugada syndrome, cardiac conduction disease, or

Table 3. GALA and Gaussian Analyses of Helix Orientations and Dynamics Using Ala-CD$_3$ |$\Delta\nu_q$| Magnitudes of GWALP23 Family Peptides[a]

lipid	peptide	pH	GALA				Gaussian					ref
			τ_0	ρ_0	S_{zz}	RMSD	τ_0	ρ_0	$\sigma\rho$	$\sigma\tau$	RMSD	
DLPC	GWALP23	--[b]	21°	305°	0.71	0.7 kHz	23°	304°	33°	5°[c]	0.7 kHz	16
	R^{14}GWALP23	--[b]	27°	259°	0.83	1.6	25°	260°	5°	5°[c]	1.6	19, this work
	R^{14}E^{16}GWALP23	6.4	10°	234°	0.82	1.1	12°	233°	36°	5°[c]	0.95	this work
DMPC	GWALP23	--	9°	311°	0.88	1.0	13°	308°	44°	5°[c]	1.1	38
	R^{14}GWALP23	--	25°	252°	0.79	1.3	26°	252°	28°	5°[c]	1.0	19, this work
	R^{14}E^{16}GWALP23	6.4	10°	232°	0.78	1.2	11°	232°	40°	5°[c]	1.3	this work
DOPC	GWALP23	--	6°	323°	0.87	0.6	9°	321°	48°	5°[c]	0.7	16
	R^{14}GWALP23	--	16°	246°	0.89	1.0	17°	246°	5°	5°[c]	1.2	19, this work
	R^{14}E^{16}GWALP23	2.4	8°	212°	0.9	2.2	10°	212°	24°	5°[c]	2.2	this work

[a]The modified Gaussian analysis followed Sparks et al.,[16] with S_{zz} fixed at 0.88 and $\sigma\tau$ fixed at 5°. [b]The helix of GWALP23 has no ionizable residues, so its tilt does not change with pH. The Arg in R^{14}GWALP23 retains its positive charge under all conditions throughout the experimental pH range, so its tilt also does not change with pH. [c]Fixed value.
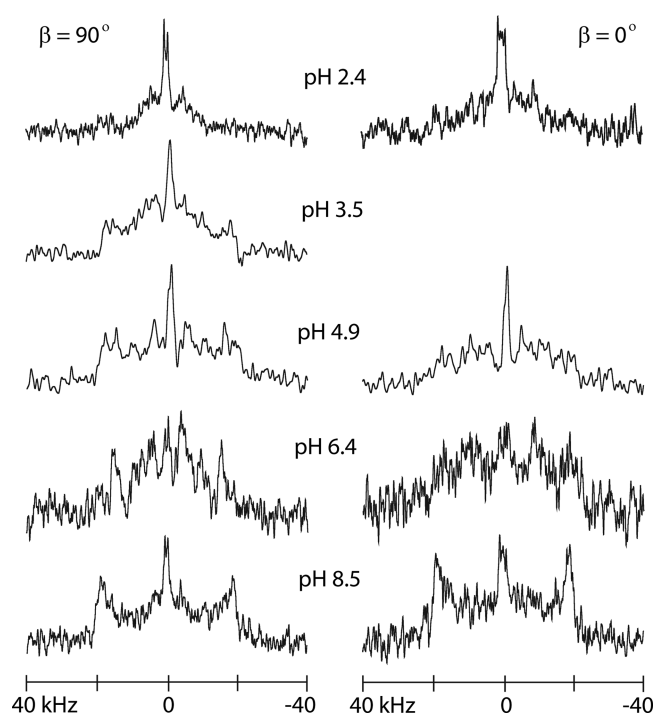

Figure 5. Deuterium NMR spectra for R^{14}E^{16}GWALP23 in differing pH conditions in the DOPC lipid bilayer. Spectra for $\beta = 90°$ (left) and $\beta = 0°$ (right) sample orientations are displayed. The ^{2}H-labeled alanines are A11 and A13; temperature, 50 °C; 1:60, peptide:lipid.

sudden infant death syndrome.[26] A distal Arg-Glu interaction alters domain associations in brain ApoE4, a component of high-density lipoprotein and a major regulator of lipid metabolism in the central nervous system. The Arg-Glu influence may lead to lower levels of ApoE4 in neuronal cells, which in turn would diminish cholesterol transport and contribute to neurodegenerative disorders such as Alzheimer's disease.[27] As a further example of conformational regulation, the gating of sodium channels in response to voltage changes is enabled by at least four Arg residues, which switch their interactions with several neighboring Glu and Asp residues, leading to the rotation, tilting, and translocation of a voltage-sensing helix.[28,29] Domain rearrangements, whether subtle or extensive, are significant for function.

Membrane association of disordered protein domains has been characterized as "semi-specific",[9] to be contrasted with explicit binding at a defined interface. The semi-specific association can be driven by weak attractive forces such as hydrogen bonding and van der Waals interactions that involve dynamic local molecular rearrangements. The bound and unbound states therefore may both retain diverse members within their populations.[9]

The context of the present work elucidates the impact of a single individual residue within a framework whose baseline structure is helical and well defined. The parent framework for the helix of R^{14}GWALP23 is especially well structured in bilayer membranes,[17,19] giving sharp ^{2}H NMR signals that arise from a well-defined helix orientation along with rapid cone precession about the bilayer normal. Additional motions arising from helix wobble $\sigma\tau$ or rotational slippage $\sigma\rho$ about the helix axis also are averaged rapidly on the NMR time scale. The introduction of E16 into the framework is dramatic. The averaging slows, broadening the ^{2}H resonance signals; new states appear, increasing the number of signals, even at low pH. As the pH increases, more signals appear until an apparent endpoint is reached near pH 8 involving a disordered aggregate of immobilized states indicated by a spectral Pake pattern. Partial unwinding of the helix terminals is anticipated,[30] even for the parent R14 helix, with the extent of fraying notably depending on the identities and ionization states of particular residues near the membrane interface.[20,31−33] While small changes in the local fraying are detected easily by the highly sensitive ^{2}H NMR methods, such changes involving helix terminal disorder may not necessarily be reflected in the circular dichroism spectra.[20,31] Notably, the helix disorder, whether arising from changes in end fraying or orientations of the core helix, is lipid-dependent as well as pH-dependent as the detailed behavior varies among bilayers of DLPC, DMPC, and DOPC. These features will be important for understanding the plasticity of protein functional domains for which, notably, the cholesterol content also is a significant regulatory factor.[23,34,35]

While induced by E16, the disorder in the R^{14}E^{16}GWALP23 population can be attributed to both residues E16 and R14 and their possible interactions and influence upon the core helix orientations and terminal fraying. When E16 is present without R14, the ^{2}H resonances are broad[20] yet the number of states remains few. When R14 is present without E16, the ^{2}H resonances are very sharp[17,19] and the core helix exhibits a single unique state in each bilayer membrane. Moreover, it is the combination of E16 with R14 that that gives rise to

disorder involving the plethora of states. The endpoint involving the Pake pattern at high pH suggests that the intermolecular ionic attraction between Glu and Arg may be significant. Each of the charged residues plays a role as the number of states and the tendency toward aggregation both are diminished when the Glu residue is neutral at low pH.

Residue interactions indeed are a likely general feature with respect to membrane protein order/disorder transitions. For the *Mycobacterium tuberculosis* ChiZ protein, interactions between Arg residues and acidic POPG lipids are significant for defining the domain disorder and membrane association.[9] More generally, membrane association often may involve amphipathic helices that can "fold upon binding".[8] A repeating consensus motif of KTKEGV is especially important for the structural plasticity of α-synuclein.[8] Mutations such as Gly to Asp as well as phosphorylation or acetylation events furthermore may influence ionic interactions, structural properties, membrane association, and physiological function.[8] Although initially framed as a straightforward example, the present work illustrates a surprising complexity of even pairwise residue interactions, not to mention the multiple steps along pathways to higher-order interactions.

■ CONCLUSIONS

We illuminate conditions under which single Glu and Arg residues introduce disorder into an otherwise stable transmembrane helix. Local variations in terminal unraveling and lipid interactions on opposite faces of a protein helix as well as intermolecular charge-mediated helix–lipid or helix–helix interactions are likely to play significant roles. The results highlight some of the complexities of order/disorder transitions among membrane proteins.

■ MATERIALS AND METHODS

Lipids were from Avanti Polar Lipids (Alabaster, AL), and deuterated alanine (Ala-d$_4$) was from Cambridge Isotope Labs (Tewksbury, MA). Ala-d$_4$ was protected by manual derivatization with an *N*-fluorenylmethoxycarbonyl (Fmoc) group and recrystallized from ethyl acetate/hexane, 80/20, as described previously.[36] Solid-phase peptide synthesis was carried out as previously[37] on a 0.1 mmol scale using an Applied Biosystems 433A synthesizer from Life Technologies (Foster City, CA). N-Fmoc amino acids with additional side-chain protections were purchased from NovaBiochem (San Diego, CA). Glutamic acid with *t*-butyl ester, arginine with 2,2,4,6,7-pentamethyl-dihydrobenzofuran-5-sulfonyl, and tryptophan with *t*-butoxy-carbonyl protecting groups were used. The cleavage of protecting groups and of peptides from a Rink amide resin (NovaBiochem) was achieved using trifluoroacetic acid to yield an amidated C-terminal. Two Ala-d$_4$ residues with differing isotopic abundances were incorporated in each synthetic sample of R^{14}E^{16}GWALP23 (Table 1), according to previous methods.[11,37]

Following completion of synthesis, peptides were cleaved from resin using a trifluoroacetic acid (TFA) cocktail composed of an 85:5:5:5 TFA:triisopropylsilane:H$_2$O:phenol ratio (v/v, w/v for phenol). After filtration of the cleavage mixture, a crude peptide was precipitated using a 50:50 mixture of hexane:(methyl, *t*-butyl ether) and lyophilized from a 50:50 mixture of acetonitrile:water. Peptides were purified by reversed-phase high-performance liquid chromatography (HPLC) on an octyl-silica column (Zorbax Rx-C8, 9.4 ×

250 mm, 5 μm particle size; Agilent Technologies, Santa Clara, CA) using a gradient of 88–92% methanol, with 0.1% trifluoroacetic acid over 30 min. Examples of the HPLC purification profile and MALDI-TOF analysis to confirm peptide identity are provided in Figures S1 and S2 of the Supporting Information. The chromatographic purification removed traces of incompletely synthesized shorter peptides as well as any residual trifluoroacetic acid.

Solid-state NMR experiments were performed using mechanically aligned peptide-lipid samples (1:60 mol:mol) prepared as described[13,38] using DLPC, DMPC, or DOPC for individual samples. Peptide-lipid films were deposited on thin glass slides from 95% methanol, dried under vacuum (10^{-4} Torr for 48 h), and hydrated (45%, w/w) with deuterium-depleted water (Cambridge Isotope Laboratories, Andover, MA) containing 20 mM glycine, citrate, or tris buffer at a specific pH value between 2.4 and 8.[23,39] The hydrated slides were stacked in 8 mm cuvettes, sealed with epoxy, and incubated at 40 °C for at least 48 h to promote bilayer alignment. Alignment was confirmed by ^{31}P NMR at 121.5 MHz using a Bruker Avance spectrometer with broadband ^{1}H decoupling (4.2 kHz). Deuterium (^{2}H) NMR experiments were performed at 46 MHz using a 300 MHz Bruker Avance spectrometer with a solid quadrupolar-echo pulse sequence[40] with a 3.0 μs 90° pulse length, a 90 ms recycle delay, and 115 μs echo delay. The spectra were recorded using 0.9–1.4 million scans and were processed with 100 Hz line broadening.

In many cases, multiple Ala methyl CD$_3$ peaks were detected, indicating multiple states (see the Results section). For samples where the Ala methyl CD$_3$ resonances could be assigned, the tilt of the core helix was estimated from the ^{2}H Ala quadrupolar splittings using a semi-static "geometric analysis of labeled alanines" ("GALA") method.[13,41] Backbone C$_\alpha$ deuterons also were present but were not detected or assigned. The results for helix orientations were confirmed by an independent modified Gaussian analysis.[16,42] In principle, either the tilt of the core helix or the multiplicity of states could show a pH dependence. Because the arginine R14 side chain is always charged,[23] the side chain of E16 is the only titratable group in the R^{14}E^{16}GWALP23 peptide sequence (Table 1).

■ ASSOCIATED CONTENT

ⓢ Supporting Information

The Supporting Information is available free of charge at https://pubs.acs.org/doi/10.1021/acsomega.1c02800.

Chromatograms, mass spectra, and graph of pH dependence (PDF)

■ AUTHOR INFORMATION

Corresponding Author

Roger E. Koeppe, II — *Department of Chemistry and Biochemistry, University of Arkansas, Fayetteville, Arkansas 72701, United States;* ⓞ orcid.org/0000-0003-0676-6413; Email: rk2@uark.edu

Authors

Jake R. Price — *Department of Chemistry and Biochemistry, University of Arkansas, Fayetteville, Arkansas 72701, United States*

Fahmida Afrose — *Department of Chemistry and Biochemistry, University of Arkansas, Fayetteville, Arkansas 72701, United States*

Denise V. Greathouse − *Department of Chemistry and Biochemistry, University of Arkansas, Fayetteville, Arkansas 72701, United States;* ● orcid.org/0000-0001-7104-8499

Complete contact information is available at:
https://pubs.acs.org/10.1021/acsomega.1c02800

Author Contributions

The manuscript was written through contributions of all authors. All authors have given approval to the final version of the manuscript.

Notes

The authors declare no competing financial interest.

■ ACKNOWLEDGMENTS

■ ABBREVIATIONS

DLPC, 1,2-dilauroyl-*sn*-glycero-3-phosphocholine; DMPC, 1,2-dimyristoyl-*sn*-glycero-3-phosphocholine; DOPC, 1,2-dioleoyl-*sn*-glycero-3-phosphocholine; Fmoc, fluorenylmethoxycarbonyl; TFA, trifluoroacetic acid; GALA, geometric analysis of labeled alanines; GWALP23, acetyl-GGALW-(LA)$_6$LWLAGA-amide; RMSD, root-mean-square deviation

■ REFERENCES

(1) Kendrew, J. C. The Three-Dimensional Structure of a Protein Molecule. *Sci. Am.* **1961**, *205*, 96−110.

(2) Phillips, D. C. The Three-Dimensional Structure of an Enzyme Molecule. *Sci. Am.* **1966**, *215*, 78−90.

(3) Sigler, P. B. Transcriptional Activation - Acid Blobs and Negative Noodles. *Nature* **1988**, *333*, 210−212.

(4) Wright, P. E.; Dyson, H. J. Intrinsically Unstructured Proteins: Re-Assessing the Protein Structure-Function Paradigm. *J. Mol. Biol.* **1999**, *293*, 321−331.

(5) Uversky, V. N.; Gillespie, J. R.; Fink, A. L. Why Are "Natively Unfolded" Proteins Unstructured under Physiologic Conditions? *Proteins: Struct. Funct., Bioinf.* **2000**, *41*, 415−427.

(6) Wright, P. E.; Dyson, H. J. Intrinsically Disordered Proteins in Cellular Signalling and Regulation. *Nat. Rev. Mol. Cell Biol.* **2015**, *16*, 18−29.

(7) Pricer, R.; Gestwicki, J. E.; Mapp, A. K. From Fuzzy to Function: The New Frontier of Protein Protein Interactions. *Acc. Chem. Res.* **2017**, *50*, 584−589.

(8) Das, T.; Eliezer, D. Membrane Interactions of Intrinsically Disordered Proteins: The Example of Alpha-Synuclein. *Biochim. Biophys. Acta* **2019**, *1867*, 879−889.

(9) Hicks, A.; Escobar, C. A.; Cross, T. A.; Zhou, H.-X. Fuzzy Association of an Intrinsically Disordered Protein with Acidic Membranes. *JACS Au* **2021**, *1*, 66−78.

(10) Vostrikov, V. V.; Grant, C. V.; Daily, A. E.; Opella, S. J.; Koeppe, R. E., II Comparison of "Polarization Inversion with Spin Exchange at Magic Angle" and "Geometric Analysis of Labeled Alanines" Methods for Transmembrane Helix Alignment. *J. Am. Chem. Soc.* **2008**, *130*, 12584−12585.

(11) Vostrikov, V. V.; Daily, A. E.; Greathouse, D. V.; Koeppe, R. E., II Charged or Aromatic Anchor Residue Dependence of Transmembrane Peptide Tilt. *J. Biol. Chem.* **2010**, *285*, 31723−31730.

(12) Koeppe, R. E., 2nd; Killian, J. A.; Greathouse, D. V. Orientations of the Tryptophan 9 and 11 Side Chains of the Gramicidin Channel Based on Deuterium Nuclear Magnetic Resonance Spectroscopy. *Biophys. J.* **1994**, *66*, 14−24.

(13) van der Wel, P. C. A.; Strandberg, E.; Killian, J. A.; Koeppe, R. E., II Geometry and Intrinsic Tilt of a Tryptophan-Anchored Transmembrane α-Helix Determined by ^{2}H NMR. *Biophys. J.* **2002**, *83*, 1479−1488.

(14) Lee, J.; Im, W. Transmembrane Helix Tilting: Insights from Calculating the Potential of Mean Force. *Phys. Rev. Lett.* **2008**, *100*, No. 018103.

(15) Strandberg, E.; Esteban-Martin, S.; Salgado, J.; Ulrich, A. S. Orientation and Dynamics of Peptides in Membranes Calculated from ^{2}H-NMR Data. *Biophys. J.* **2009**, *96*, 3223−3232.

(16) Sparks, K. A.; Gleason, N. J.; Gist, R.; Langston, R.; Greathouse, D. V.; Koeppe, R. E., II Comparisons of Interfacial Phe, Tyr, and Trp Residues as Determinants of Orientation and Dynamics for GWALP Transmembrane Peptides. *Biochemistry* **2014**, *53*, 3637−3645.

(17) Vostrikov, V. V.; Hall, B. A.; Greathouse, D. V.; Koeppe, R. E., II; Sansom, M. S. P. Changes in Transmembrane Helix Alignment by Arginine Residues Revealed by Solid-State NMR Experiments and Coarse-Grained MD Simulations. *J. Am. Chem. Soc.* **2010**, *132*, 5803−5811.

(18) Vostrikov, V. V.; Grant, C. V.; Opella, S. J.; Koeppe, R. E., II On the Combined Analysis of ^{2}H and ^{15}N/^{1}H Solid-State NMR Data for Determination of Transmembrane Peptide Orientation and Dynamics. *Biophys. J.* **2011**, *101*, 2939−2947.

(19) Vostrikov, V. V.; Hall, B. A.; Sansom, M. S. P.; Koeppe, R. E., II Accommodation of a Central Arginine in a Transmembrane Peptide by Changing the Placement of Anchor Residues. *J. Phys. Chem. B* **2012**, *116*, 12980−12990.

(20) Rajagopalan, V.; Greathouse, D. V.; Koeppe, R. E., II Influence of Glutamic Acid Residues and pH on the Properties of Transmembrane Helices. *Biochim. Biophys. Acta, (BBA) - Biomembranes* **2017**, *1859*, 484−492.

(21) Killian, J. A.; Taylor, M. J.; Koeppe, R. E., II Orientation of the Valine-1 Side-Chain of the Gramicidin Transmembrane Channel and Implications for Channel Functioning. A deuterium NMR study. *Biochemistry* **1992**, *31*, 11283−11290.

(22) Gleason, N. J.; Vostrikov, V. V.; Greathouse, D. V.; Koeppe, R. E., II Buried Lysine, but Not Arginine, Titrates and Alters Transmembrane Helix Tilt. *Proc. Natl. Acad. Sci. U. S. A.* **2013**, *110*, 1692−1695.

(23) Thibado, J. K.; Martfeld, A. N.; Greathouse, D. V.; Koeppe, R. E., II Influence of High pH and Cholesterol on Single Arginine-Containing Transmembrane Peptide Helices. *Biochemistry* **2016**, *55*, 6337−6343.

(24) Yeung, T.; Terebiznik, M.; Yu, L.; Silvius, J.; Abidi, W. M.; Philips, M.; Levine, T.; Kapus, A.; Grinstein, S. Receptor Activation Alters Inner Surface Potential During Phagocytosis. *Science* **2006**, *313*, 347−351.

(25) Haxholm, G. W.; Nikolajsen, L. F.; Olsen, J. G.; Fredsted, J.; Larsen, F. H.; Goffin, V.; Pedersen, S. F.; Brooks, A. J.; Waters, M. J.; Kragelund, B. B. Intrinsically Disordered Cytoplasmic Domains of Two Cytokine Receptors Mediate Conserved Interactions with Membranes. *Biochem. J.* **2015**, *468*, 495−506.

(26) Yu, G.; Liu, Y.; Qin, J.; Wang, Z.; Hu, Y.; Wang, F.; Li, Y.; Chakrabarti, S.; Chen, Q.; Wang, Q. K. Mechanistic Insights into the Interaction of the Mog1 Protein with the Cardiac Sodium Channel Nav1.5 Clarify the Molecular Basis of Brugada Syndrome. *J. Biol. Chem.* **2018**, *293*, 18207−18217.

(27) Mahley, R. W. Central Nervous System Lipoproteins: ApoE and Regulation of Cholesterol Metabolism. *Arterioscler., Thromb., Vasc. Biol.* **2016**, *36*, 1305−1315.

(28) DeCaen, P. G.; Yarov-Yarovoy, V.; Scheuer, T.; Catterall, W. A. Gating Charge Interactions with the S1 Segment During Activation of a Na+ Channel Voltage Sensor. *Proc. Natl. Acad. Sci., U. S. A.* **2011**, *108*, 18825−18830.

(29) Yarov-Yarovoy, V.; DeCaen, P. G.; Westenbroek, R. E.; Pan, C. Y.; Scheuer, T.; Baker, D.; Catterall, W. A. Structural Basis for Gating

Charge Movement in the Voltage Sensor of a Sodium Channel. *Proc. Natl. Acad. Sci. U. S. A.* **2012**, *109*, E93−E102.

(30) Mortazavi, A.; Rajagopalan, V.; Sparks, K. A.; Greathouse, D. V.; Koeppe, R. E., II Juxta-Terminal Helix Unwinding as a Stabilizing Factor to Modulate the Dynamics of Transmembrane Helices. *ChemBioChem* **2016**, *17*, 462−465.

(31) Afrose, F.; McKay, M. J.; Mortazavi, A.; Suresh Kumar, V.; Greathouse, D. V.; Koeppe, R. E., II Transmembrane Helix Integrity Versus Fraying to Expose Hydrogen Bonds at a Membrane-Water Interface. *Biochemistry* **2019**, *58*, 633−645.

(32) Afrose, F.; Martfeld, A. N.; Greathouse, D. V.; Koeppe, R. E., II Examination of pH Dependency and Orientation Differences of Membrane Spanning Alpha Helices Carrying a Single or Pair of Buried Histidine Residues. *Biochim. Biophys. Acta, (BBA) - Biomembranes* **2021**, *1863*, 183501.

(33) McKay, M. J.; Marr, K. A.; Price, J. R.; Greathouse, D. V.; Koeppe, R. E., II Lipid-Dependent Titration of Glutamic Acid at a Bilayer Membrane Interface. *ACS Omega* **2021**, *6*, 8488−8494.

(34) Frey, L.; Hiller, S.; Riek, R.; Bibow, S. Lipid- and Cholesterol-Mediated Time-Scale-Specific Modulation of the Outer Membrane Protein X Dynamics in Lipid Bilayers. *J. Am. Chem. Soc.* **2018**, *140*, 15402−15411.

(35) Lipinski, K.; McKay, M. J.; Afrose, F.; Martfeld, A. N.; Koeppe, R. E., II; Greathouse, D. V. Influence of Lipid Saturation, Hydrophobic Length and Cholesterol on Double-Arginine-Containing Helical Peptides in Bilayer Membranes. *ChemBioChem* **2019**, *20*, 2784−2792.

(36) Thomas, R.; Vostrikov, V. V.; Greathouse, D. V.; Koeppe, R. E., II Influence of Proline Upon the Folding and Geometry of the WALP19 Transmembrane Peptide. *Biochemistry* **2009**, *48*, 11883−11891.

(37) Gleason, N. J.; Vostrikov, V. V.; Greathouse, D. V.; Grant, C. V.; Opella, S. J.; Koeppe, R. E., II Tyrosine Replacing Tryptophan as an Anchor in GWALP Peptides. *Biochemistry* **2012**, *51*, 2044−2053.

(38) McKay, M. J.; Martfeld, A. N.; De Angelis, A. A.; Opella, S. J.; Greathouse, D. V.; Koeppe, R. E., II Control of Transmembrane Helix Dynamics by Interfacial Tryptophan Residues. *Biophys. J.* **2018**, *114*, 2617−2629.

(39) Martfeld, A. N.; Greathouse, D. V.; Koeppe, R. E., II Ionization Properties of Histidine Residues in the Lipid Bilayer Membrane Environment. *J. Biol. Chem.* **2016**, *291*, 19146−19156.

(40) Davis, J. H.; Jeffrey, K. R.; Bloom, M.; Valic, M. I.; Higgs, T. P. Quadrupolar Echo Deuteron Magnetic Resonance Spectroscopy in Ordered Hydrocarbon Chains. *Chem. Phys. Lett.* **1976**, *42*, 390−394.

(41) McKay, M. J.; Fu, R.; Greathouse, D. V.; Koeppe, R. E., II Breaking the Backbone: Central Arginine Residues Induce Membrane Exit and Helix Distortions within a Dynamic Membrane Peptide. *J. Phys. Chem. B* **2019**, *123*, 8034−8047.

(42) Strandberg, E.; Esteban-Martín, S.; Ulrich, A. S.; Salgado, J. Hydrophobic Mismatch of Mobile Transmembrane Helices: Merging Theory and Experiments. *Biochim. Biophys. Acta* **2012**, *1818*, 1242−1249.